

CATPlan: Loss-based Collision Prediction in End-to-End Autonomous Driving

Ziliang Xiong¹, Shipeng Liu¹, Nathaniel Helgesen¹, Joakim Johnander², Per-Erik Forssén¹
Computer Vision Laboratory, Department of Electrical Engineering, Linköping University¹
Zenseact, Sweden²
{name.surname}@liu.se, {name.surname}@zenseact.com

Abstract

In recent years, there has been increased interest in the design, training, and evaluation of end-to-end autonomous driving (AD) systems. One often overlooked aspect is the uncertainty of planned trajectories predicted by these systems, despite awareness of their own uncertainty being key to achieve safety and robustness. We propose to estimate this uncertainty by adapting loss prediction from the uncertainty quantification literature. To this end, we introduce a novel light-weight module, dubbed CATPlan, that is trained to decode motion and planning embeddings into estimates of the collision loss used to partially supervise end-to-end AD systems. During inference, these estimates are interpreted as collision risk. We evaluate CATPlan on the safety-critical, nerf-based, closed-loop benchmark NeuroNCAP and find that it manages to detect collisions with a 54.8% relative improvement to average precision over a GMM-based baseline in which the predicted trajectory is compared to the forecasted trajectories of other road users. Our findings indicate that the addition of CATPlan can lead to safer end-to-end AD systems and hope that our work will spark increased interest in uncertainty quantification for such systems.

1. Introduction

Robust and reliable uncertainty estimation is one of the holy grails of autonomous driving (AD) perception systems. In the presence of uncertainty, the AD system can, e.g., decrease speed or hand over to the driver. Moreover, sensor data can be transmitted to the cloud for analysis and to be used to train future versions of the AD perception system in an active learning paradigm [11, 35].

In recent years, a number of works [17, 20] propose end-to-end planners that map sensor input to trajectories that the ego-vehicle should follow. These systems can be compared to traditional modular software stacks with engineered interfaces between modules and handcrafted rules. The end-to-end planner has a number of advantages [17, 29]. They

do not suffer from information loss between different parts of the system due to engineered interfaces, e.g., between a detector and tracker. Instead, different parts of the system learn what information to pass based on training data. This enables the end-to-end planner to, for instance, capture cues that reveal the intent of other road users. Moreover, these methods are expected to have a human-like driving behavior, learned by letting the predicted trajectories imitate that of human drivers. However, an open question is how safety can be guaranteed in such systems.

As a vital step towards safe end-to-end planners, we are interested in the uncertainty of the planned trajectories. The literature on uncertainty quantification provides a variety of approaches, but one that is particularly appealing is *loss prediction* [40]. The critical failure in an end-to-end planner is that a planned trajectory leads to a collision. These methods are therefore partially supervised by a collision loss during training. The collision loss penalizes planned trajectories that are too close to recorded trajectories of other objects [17, 20]. The idea in loss prediction is to capture uncertainty through a small neural network trained to map deep features to an estimate of the loss function, in our case, the collision loss. The question we try to answer in this work is whether loss-prediction works for end-to-end planners, which are complex neural networks supervised by a large number of loss functions, with one of these losses being of primary interest.

To this end, We introduce a novel lightweight module, which we dub Collision Alert Transformer for Planning (CATPlan), for predicting collision risk for the plan end-to-end planners. CATPlan is trained to decode the motion and planning queries from a given AD model into the collision loss value, which can be interpreted during inference as a confidence value on the binary collision prediction. We evaluate CATPlan in safety-critical scenarios—e.g., a vehicle coming from a side of the ego-vehicle—through the NeuroNCAP [29] benchmark. NeuroNCAP is a closed-loop simulator with scenarios that look realistic due to neural rendering of recorded logs. As a real-world evaluation benchmark, we use nuScenes [3]. While nuScenes contains

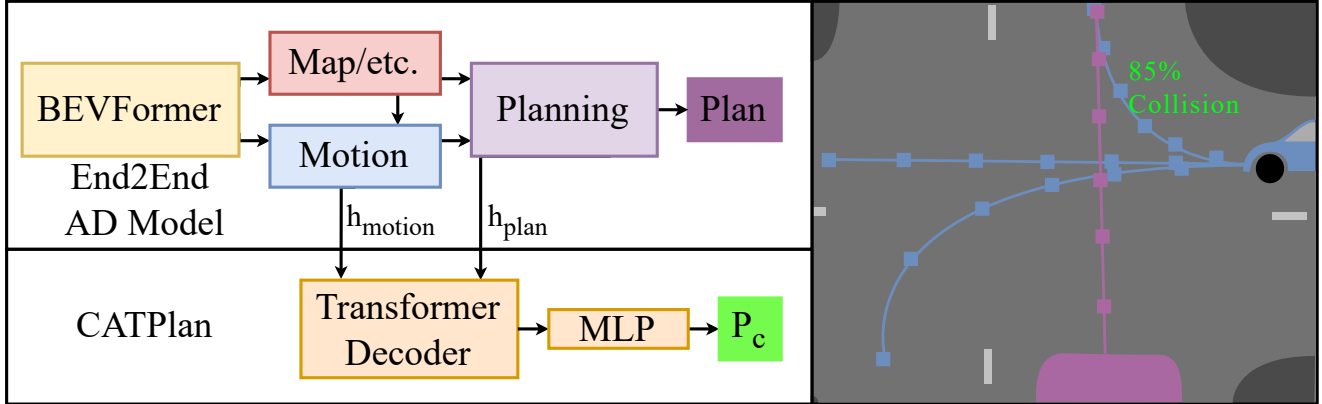


Figure 1. Basic synopsis of the CATPlan model. While conventional End-to-End Autonomous Driving Models output a plan for the vehicle to enact, our model is trained on the embeddings from such models and outputs the probability of a collision happening during that planned route. This can enable a self-driving vehicle to take emergency action or switch to driver assistance.

normal driving logs rather than safety-critical scenarios and does not allow for closed-loop evaluation, it contains purely realistic data without artifacts induced by neural rendering. Through extensive evaluation, we show that CATPlan outperforms the rule-based baseline by 54.76% on the simulated data and 151.2% on the real-world data.

We summarize our main **contributions** as the following:

1. We introduce the collision alert transformer for planners, CATPlan, to predict the confidence of collision for planned trajectories; a novel approach to uncertainty estimation in autonomous driving systems.
2. We show that loss prediction is applicable to substantially more complex models than what has been previously tested. Besides, we show loss prediction could be treated as a classification task instead of a regression task compared to what has been tested before.
3. Through extensive evaluation, our lightweight CATPlan module manages to capture 50% of all collisions with a precision of 45.6% in real-world datasets. We further reveal that the bottleneck of performance is the domain gap between different AD video sequences.

2. Related Work

End-to-End Autonomous Driving: Different sub-tasks of autonomous driving perception has been studied extensively, e.g., object detection [9, 26, 28], bird’s-eye-view (BEV) segmentation [13, 34], object tracking [6, 25, 31, 32], and motion forecasting [1, 14, 18, 19]. End-to-end planning was studied both in the CARLA [10] closed-loop simulator [4, 7, 33, 39] and on real data [15, 16, 22]. Hu et al. [17] aim to secure the advantages of both a modular stack and an end-to-end planner. To this end, they propose a modular method—comprising a BEV-encoder [26], a combined detector and tracker [31], a map encoder, a motion forecaster, an occupancy grid estimation module, and

a planner—where the information flow between different modules is learned end-to-end. A few works follow a similar design philosophy. Jiang et al. [20] propose a more computationally efficient architecture. Chen et al. [5] propose to interleave prediction and planning at every timestep of forecasting. Zheng et al. [45] propose to view autonomous driving as a trajectory generation problem.

Uncertainty Quantification in Autonomous Driving: Autonomous driving is safety-critical and it is generally believed that predictive uncertainty estimation is essential [12, 37]. In what is widely considered to be the seminal work in the field of uncertainty quantification in neural networks, Kendall and Gal [21] analyze the uncertainty in the prediction of a neural network by decomposing it into aleatoric and epistemic uncertainty. Aleatoric uncertainty stems from the stochastic nature of the data and is therefore irreducible. Epistemic uncertainty stems from the lack of knowledge of the model and is therefore reducible after collecting more training data. AD perception systems often model aleatoric uncertainty to some extent. Object detectors provide uncertainty estimates, which are aleatoric, on the existence of each detection and in some works on the object state as well [2, 44]. Trajectory forecasting methods typically model future object states probabilistically [1, 8, 14]. Some works estimate epistemic uncertainty, using, e.g., ensembles or monte carlo dropout [30, 41]. In contrast to earlier works, we propose to focus on the estimation of uncertainty that risks leading to unsafe behavior. To that end, we focus on collision risk.

Loss Prediction: Yoo and Kweon [40] proposed a loss prediction module, which they used for task-agnostic active learning. Their method was evaluated for tasks including image classification, object detection, and human pose estimation. Kirchhof et al. [23] proposes a benchmark for transferable uncertainty estimation and compares

eleven uncertainty quantifiers pretrained on ImageNet, including a loss-prediction model pretrained on a classical cross-entropy classification objective. They conclude that estimating the prediction loss directly outperforms unsupervised uncertainty estimate techniques. Yu et al. [42] proposes a discretization-induced Dirichlet posterior for robust uncertainty quantification on regression. In the work of Yu et al. [42], there are two separate auxiliary models and the aleatoric uncertainty is predicted in loss prediction fashion. In this work, we adopt loss prediction to the collision loss component to detect plans that would lead to a collision. This loss component is one out of many losses used to supervise end-to-end planners. Moreover, as we argue in Sec. 3, we are primarily interested in whether there is a collision, not the size of the loss. Thus, the loss prediction task is framed as binary classification rather than regression.

3. Method

We first review the theory of loss prediction in Sec. 3.1. Then we adapt this to collision prediction for end-to-end planning in Sec. 3.2. Next, we introduce our CATPlan architecture in Sec. 3.3 and a rule-based collision model as the baseline in Sec. 3.4. Finally, we introduce techniques for handling class imbalance in real-world data in Sec. 3.5.

3.1. Preliminaries: Loss Prediction

The core idea of loss prediction is to add an auxiliary module to some target model Θ_{target} [40], for instance, an image classifier, to predict its loss value as an indicator of prediction uncertainty. Given a training sample \mathbf{x} , we obtain a target prediction \hat{y} and intermediate features h_i through the target model as

$$\hat{y}, h_1, \dots, h_n = \Theta_{\text{target}}(\mathbf{x}) , \quad (1)$$

$$h = \{h_1, h_2, \dots, h_n\}, n \geq 1 , \quad (2)$$

$$L_{\text{target}} = \mathcal{L}_{\text{target}}(\hat{y}, y) . \quad (3)$$

The target loss value L_{target} can be computed with the annotation y of the sample \mathbf{x} as in Eq. (3). Meanwhile, the auxiliary module Θ_{loss} predicts the loss value of the target model with the set of features h as the input as described in Eq. (4). Given the target loss value L_{target} is a ground-truth target of h for the loss prediction Θ_{loss} , we can compute the auxiliary loss value as

$$\hat{L}_{\text{target}} = \Theta_{\text{loss}}(h) , \quad (4)$$

$$L_{\text{loss}} = \mathcal{L}_{\text{loss}}(\hat{L}_{\text{target}}, L_{\text{target}}) . \quad (5)$$

Formally, we write the total loss function used to train the target model Θ_{target} and the loss prediction module Θ_{loss} as

$$\mathcal{L}_{\text{target}}(\hat{y}, y) + \lambda \mathcal{L}_{\text{loss}}(\hat{L}_{\text{target}}, L_{\text{target}}) , \quad (6)$$

where λ is a predefined constant scaling factor.

To avoid Θ_{loss} from interfering with Θ_{target} during training, Kirchof et al. [24] proposed to stop the gradient being back-propagated to Θ_{target} . Moreover, to speed up training, h and L_{target} are cached during the training of Θ_{target} , and Θ_{loss} is then trained separately.

After training, the loss prediction module Θ_{loss} becomes an uncertainty quantifier by letting a higher predicted value mean that the target model is more uncertain [23]. Next, we extend loss prediction to predict whether modern end-to-end planners will generate colliding trajectories.

3.2. Collision Prediction

As we argue in Sec. 1, for driving safety, we are particularly interested in predicting whether the planned trajectory will cause a collision. To train CATPlan, we first need to determine which loss value in the end-to-end AD model should be used as the training label \hat{L}_{target} and which features to include in the input set h . We address these two questions in the following section.

Choice of target loss: In contrast to target models tested in previous works of loss prediction, state-of-the-art end-to-end planners are much larger and more complex. They comprise multiple modules designed to handle different tasks such as tracking, mapping, motion prediction, and planning. There is no single loss as in standard loss prediction tasks; instead, different modules have their own loss functions and each such loss-function can comprise multiple parts. Moreover, modules that are transformers often repeat the loss functions for each layer in the transformer. Thus, there are a large number of loss components.

For training CATPlan, we focus on the collision loss component present in the planning module. The planning module loss function comprises multiple parts, including an imitation loss $\mathcal{L}_{\text{imitation}}$ and a collision loss $\mathcal{L}_{\text{collision}}$. The imitation loss is usually the L_1 or L_2 distance to the ground truth trajectory so that the model learns to exhibit human-like planning capability, while the collision loss penalizes plans that result in collisions with other agents on the road. To apply loss prediction, we adopt the collision loss component for the last transformer layer, $\mathcal{L}_{\text{collision}}$, and train Θ_{loss} to predict its value.

The scale of $L_{\text{collision}}$ does not necessarily indicate the severity of collisions in the physical world because it does not take speed into account. Therefore, it is not optimal to treat collision prediction as a regression task as is standard in loss prediction [24, 40]. Instead, we note that the sign of the collision loss indicates whether a collision is going to happen along the planned trajectory.¹ Thus, it is natural to instead treat collision prediction as a binary classification task and predict the probability of a collision occurring

¹See Eq. (4) in VAD [20] for example.

along the planned trajectory $\hat{\tau}_{\text{plan}}$,

$$P(\text{collision} \mid \hat{\tau}_{\text{plan}}) = \Theta_{\text{collision}}(h) . \quad (7)$$

Then CATPlan is trained using

$$L_{\text{loss}} = \mathcal{L}_{\text{collision}}(P(\text{collision} \mid \hat{\tau}_{\text{plan}}), L_{\text{collision}}) , \quad (8)$$

where $\mathcal{L}_{\text{collision}}$ is a cross-entropy loss or focal loss.

Choice of features: An open question is which features h should be fed into $\Theta_{\text{collision}}(h)$. Given a training sample \mathbf{x} , each module of the end-to-end planner produces separate predictions using many consecutive intermediate features. The baseline described in Sec. 3.4 makes use of the motion predictions $\hat{\tau}_{\text{motion}}$ and the planned ego trajectory $\hat{\tau}_{\text{plan}}$ to predict collisions. We note that this motion prediction is intentionally stochastic, as end-to-end AD models typically predict multi-modal trajectories to balance the unpredictability of the intentions of other drivers. Since both $\hat{\tau}_{\text{plan}}$ and $\hat{\tau}_{\text{motion}}$ are outputs from individual transformer modules, we can also output the respective planning query h_{plan} and agent queries h_{motion} . Because these queries are the layers directly before $\hat{\tau}_{\text{plan}}$ and $\hat{\tau}_{\text{motion}}$, they conceivably contain even more information, thus we opt to use them as the inputs for CATPlan. The effectiveness of this switch is demonstrated in Tab. 1 and Tab. 2. Formally, the outputs we cache from the end-to-end planner are

$$\hat{\tau}_{\text{plan}}, \hat{\tau}_{\text{motion}}, h_{\text{plan}}, h_{\text{motion}} = \Theta_{\text{target}}(\mathbf{x}) . \quad (9)$$

3.3. CATPlan Architecture

We then design the architecture of CATPlan based on the dimensions of these two queries. First, we take a closer look at the inputs of CATPlan. The planning query is in the shape of $h_{\text{plan}} \in \mathbb{R}^d$ and the agent query is in the shape of $h_{\text{motion}} \in \mathbb{R}^{N_a \times N_m \times d}$, where N_a is the number of agents and N_m is number of modalities. Previous work in loss prediction [23, 40] typically use a fully-connected architecture for the loss prediction module. Through our ablation in Sec. 4.3, we find this design results in inferior performance in our task. This is likely due to there being no interaction between the plan query and the agent query. Instead, we propose to use a transformer decoder to entangle the agent queries with the plan query by letting the latter cross-attend the former,

$$\mathbf{z} = \text{TransformerDecoder}(\tilde{h}_{\text{plan}}, \tilde{h}_{\text{motion}}) . \quad (10)$$

Here, we reshape the planning query as $\tilde{h}_{\text{plan}} \in \mathbb{R}^{1 \times d}$ and flatten the last two dimensions of the motion queries followed by a Linear layer and a ReLU to produce $\tilde{h}_{\text{motion}} \in \mathbb{R}^{N_a \times d}$. Finally, we pass \mathbf{z} through an MLP with a terminal sigmoid to produce the collision probability prediction,

$$\Theta_{\text{collision}}(h) = \text{MLP}(\mathbf{z}) . \quad (11)$$

The architecture is visualized in Fig. 1.

3.4. Baseline: Trajectory GMM

To evaluate the effectiveness of data-driven collision prediction, we compare it to a rule-based baseline model. Rule-based collision prediction has been widely used in the field of model predictive control (MPC)[46]. The most straightforward rule is to compare the planning trajectory with the future locations of other road users. Since the true future trajectory is not available, motion prediction is used as a proxy. In most end-to-end planners, like in [46], a Gaussian Mixture Model (GMM) is used to build each agent’s multimodal trajectory, $\hat{\tau}_{\text{motion}}$. Specifically, the trajectory of each agent consists of an ensemble of possible future trajectories with corresponding probabilities for each individual trajectory [17]. This ensemble can be used to define a rule-based collision prediction by replacing the trajectories from MPC optimization [46] with the predicted trajectories from an end-to-end AD planner. Thus our baseline will be a sequence of chained GMMs, and their maximum will be the collision risk estimate.

The planning outcome from end-to-end planners is a unimodal trajectory consisting of waypoints, $\hat{\tau}_{\text{plan}} \in \mathbb{R}^{T \times 2}$, where T is the number of predicted future waypoints and 2 corresponds to the ego-vehicle centered bird-eye view 2D coordinates. The end-to-end planner of most AD systems provides a motion prediction $\hat{\tau}_{\text{motion}} \in \mathbb{R}^{N_a \times N_m \times T \times 2}$ for each agent, in the form of an ensemble of M possible future trajectories with corresponding probabilities $\{\pi_m\}_1^M$, for each individual trajectory [17]. We let these define a chain of GMMs, one for each time step k and agent a :

$$p(x_k | t_{a,k}) = \sum_{m=1}^M \pi_m \mathcal{N}(x_k - \hat{\tau}_{\text{motion}_{a,k,m}}, \Sigma_k) \quad (12)$$

By evaluating each of these at the corresponding positions for the ego-trajectory, and taking the maximum, we obtain a straightforward baseline score that rates the risk of collision for a given ego-vehicle plan.

$$R_{\text{collision}} = \max_k p(x_k | t_{a,k}) \quad (13)$$

The covariance Σ_k is set to be the size of ego-vehicle when $k = 1$, and linearly increasing with the prediction time, i.e. $\Sigma_k = k\sigma_0 \mathbf{I}$. We then calculate the log-likelihood of the planned trajectory at each step with all the GMMs at the same steps and take the maximum as a proxy to the probability of at least one crash.

3.5. Bagging Ensemble, Mixup, and Focal Loss

Real-world AD datasets are typically imbalanced as samples without collisions greatly outnumber those with collisions. To alleviate this issue, we propose to combine the bagging ensemble and undersampling of Westny et al. [38]

with the focal loss of Lin et al. [27]. Given the set of collision samples P and a set of non-collision class examples Q , $|P| < |Q|$. In bagging, Q is split into N subsets, Q_1, Q_2, \dots, Q_N , and each subset is combined with P to form N training sets. Then, N models are trained independently with a focal loss. The final prediction is the average of the predictions of the N models. We use a focal loss with the default $\gamma = 2$ and set the class weight α to the inverse of the class ratio in each of the N bags.

$$\alpha = \frac{|Q|}{N|P| + |Q|}. \quad (14)$$

The optimal N is chosen using a validation set.

4. Experiments

To test the efficacy of our methodology, we first apply CATPlan to the safety-critical scenarios created from photo-realistic Nerf-based simulation in Sec. 4.1. Then, we evaluate the performance of CATPlan on the nuScenes dataset [3], which contains fewer safety-critical scenarios, in Sec. 4.2. Finally, we ablate the components and hyperparameters of CATPlan in Sec. 4.3.

Evaluation Metrics: Because we treat collision prediction as a binary classification problem, we use Area Under the ROC Curve (AUROC) and Average Precision (AP). The latter is also known as Area under Precision Recall Curve (AUPRC), to evaluate the performance of CATPlan. Since AP is known to be more sensitive to data imbalance, it is more suitable for real-world evaluation in Sec. 4.2. We also report the precision at recall levels of 30%, 50%, and 70%, as they can tell us how many false positives we have to accept to find a certain percentage of collisions. All metrics are better with higher values.

End-to-End AD Planners: We choose UniAD [17] and VAD [20] as the target models in this section. These models maintain state-of-the-art performance on collision avoidance and planning as shown by Zheng et al. [45], and furthermore, are shown to work in conjunction with NeuroNCAP [29], a safety-critical scenario simulator we leverage to explore how CATPlan performs on more balanced collision data. To be consistent, we cache the agent queries from the Motion Transformer module of each model, and similarly, we cache the plan query from the Planning Transformer module of each.

Collision predictor: We compare CATPlan with GMM baseline in Sec. 3.4 and a two-layer MLP model that accept the plan query as the input.

4.1. Safety-critical Scenarios

As collision samples are rare in real-world datasets, we first apply CATPlan to safety-critical scenarios via simulation. We use the SotA closed-loop simulation platform, NeuroNCAP [29], to generate a balanced dataset. In NeuroNCAP,

an end-to-end AD model receives the sensor input from NeuRAD and outputs the planned trajectory. The planned trajectory is then passed to a controller and vehicle model to move the ego vehicle forward, and afterward, NeuRAD renders the next frame of the 3D scene. In this way, it can evaluate end-to-end AD models in a closed-loop manner. NeuroNCAP uses the Nerf-based simulator of Tonderski et al. [36], NeuRAD, to generate three types of safety-critical scenarios, namely "stationary", "side", and "frontal". In the example shown in Fig. 2a, in a "side" scenario, the actor is coming toward the ego-vehicle from the left side of a crossroad. NeuRAD is trained on 10 sequences of the nuScenes validation set [3] and is able to generate diverse and realistic scenarios. For each sequence, Ljungbergh et al. [29] manually pick 1-4 actors that are nearby and determine a collision location somewhere along the ego-vehicle trajectory.

We use the same settings as Ljungbergh et al. [29] to cache the embeddings in the end-to-end AD planners. The ratio of collision samples on test set are 46%. We create the training and test datasets with a 7:3 ratio. Each contains all three types of scenarios but strictly avoids using the same sequence in both sets to diminish the chance that the model learns the sequences rather than the task. This further imitates Nuscenes which uses different sequences for the training and validation sets.

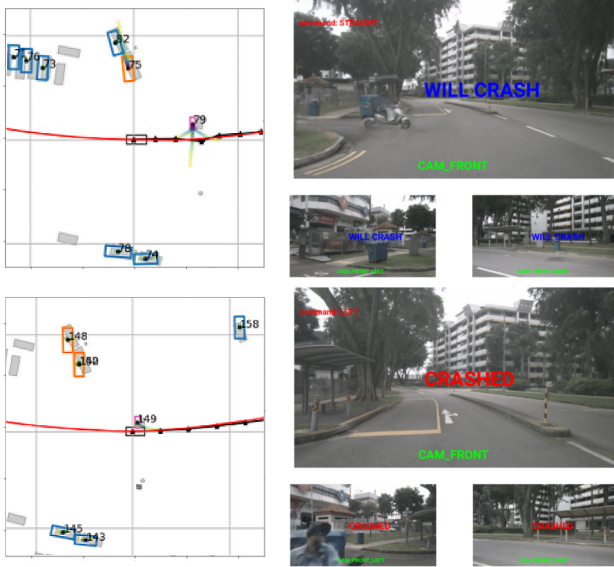
Results: The models are trained for 20 epochs with the learning rate set as 0.001, and the results are shown in Tab. 1. For the training of CATPlan and MLP, we use focal loss with $\alpha = 0.5$ and $\gamma = 2$. The qualitative examples of CATPlan are shown in Fig.2.

Model	AUROC	AP	Pr30	Pr50	Pr70	Pr100
Baseline	49.4	43.1	44.3	49.8	44.7	45.3
MLP	64.7	56.5	56.0	56.4	58.8	45.8
CATPlan	70.6	66.7	77.2	67.5	59.4	45.8

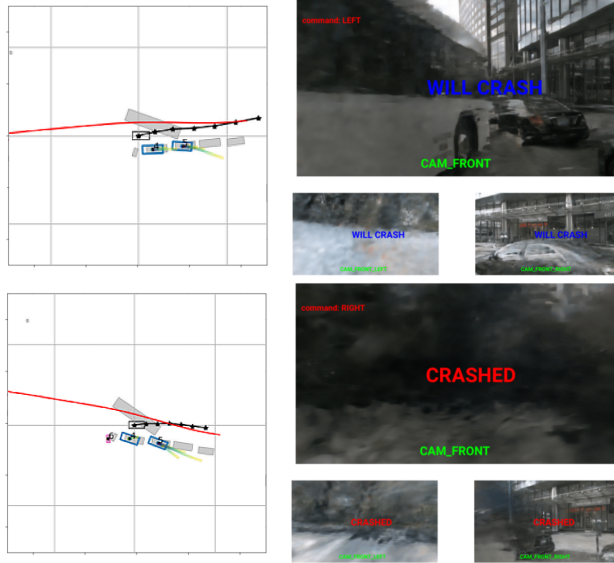
Table 1. Classification results on NeuroNCAP simulation dataset. All the values are in percentage.

Analysis: The classification results presented in Tab. 1 demonstrate the effectiveness of CATPlan in identifying potential collisions across safety-critical scenarios. The baseline achieves an AUROC of 49.4% and AP of 43.1%, indicating that its performance is close to random guessing. By contrast, the MLP-based model significantly improves the detection capability, suggesting that learning a direct mapping from h_{plan} query to collision likelihood is beneficial. CATPlan outperforms both baselines, achieving an AUROC of 70.6% and AP of 66.7%, indicating its better capability to capture collision-critical factors. This suggests that by cross-attending ego planning and agent dynamics using cross-attention, CATPlan improves collision detection for diverse simulated safety-critical scenarios.

Qualitative Examples: We present qualitative examples for true positive and false negative predictions in Fig. 2a and Fig. 2b respectively. In the left of Fig. 2b, the BEV display reveals that the UniAD model fails to detect the bus (the huge grey rectangular without blue box indicated the wrong



(a) Example of true positive prediction.



(b) Example of false negative prediction.

Figure 2. Qualitative Examples on NeuroNCAP Simulation Dataset with UniAD as the end-to-end planner. The left figure presents ground truth objects (gray) alongside predicted objects (color-coded by category) and their forecasted trajectories (blue-yellow gradient line) in the bird’s eye view. It also depicts the ego-vehicle (black), the planned trajectory (black), and the reference trajectory (red) indicating its intended turn. The right figures are the inputs of 3 front cameras.

detection result) in front of the ego vehicle. Consequently, the motion query lacks information about the bus, leading CATPlan to misclassify the scenario. This suggests that the accuracy of the perception modules in the AD model directly influences the predictive capability of CATPlan.

In contrast, in the True Positive (TP) example shown in Figure 2a, UniAD provides more accurate coordinate estimations for a nearby object (indicated by the purple box), allowing CATPlan to correctly predict the collision. Interestingly, the plan from UniAD is still going straight even if there is a detected agent coming from the side. This highlights the necessity of having collision prediction when deploying end-to-end planners for AD. This further underscores the importance of reliable perception in downstream collision forecasting, as inaccuracies in detected objects or predicted motions can propagate errors into higher-level decision-making models. These findings highlight the necessity of improving perception quality in end-to-end AD systems, as perception errors can significantly degrade downstream collision prediction.

4.2. Real-World Data

UniAD and VAD are both trained and evaluated on the real-world dataset nuScenes [3]. More specifically, both UniAD and VAD are trained on the nuScenes training split and evaluated on the validation split. The nuScenes training and validation splits contain different sequences. We cache the h_{plan} , h_{motion} and $L_{\text{collision}}$ of both planners on each split to build the training set and test set for CATPlan. In the work of Hu *et al.* [17], various levels of safety distance is used for the collision loss, which means $L_{\text{collision}} > 0$ if an agent’s distance to the ego-vehicle is within the safety distance. There is no such setting in [20], thus we transplant the collision loss of UniAD in VAD and use the same safety distance for both models. The caching process takes place during the last training epoch of the planner meaning the test-time optimization in UniAD is not used. Due to this, there are more collision samples than the collision rate reported in [17]. There are around 7.7% training samples h_{plan} , h_{motion} and 8% test samples labeled as collision class for UniAD queries. There are around 5.96% training samples h_{plan} , h_{motion} and 6.18% test samples labeled as collision class for VAD queries. The bagging ensemble described in Sec. 3.5 is used in training to help alleviate this imbalance. Specifically, we use 4 bagging ensemble and $\alpha = 0.75$ in the focal loss, mixup $\beta = 3.0$. The same batch size, optimizer, bagging ensemble, and focal loss apply to CATPlan and MLP.

Results: In Tab. 2, we evaluate the performance of the MLP and our proposed CATPlan and compare them against the GMM baseline. For UniAD queries, GMM baseline performance is merely better than random guesses. This is because the motion prediction $\hat{\tau}_{\text{motion}}$ could be inaccurately lo-

cated and the modality scores $\{\pi_l\}_1^L$ could be uncalibrated. The performance of the MLP is significantly better than the baseline and our proposed CATPlan gains the best performance. Pr50 suggests that to be able to find half of the collision samples, there are less than 70% false positive predictions. For VAD queries, we see a similar performance. Even though the VAD queries are more imbalanced, CATPlan achieves surprisingly better performances. This indicates that the quality of queries from the target model can affect CATPlan performances.

Query	Model	AUROC	AP	Pr30	Pr50	Pr70	Pr100
UniAD	Baseline	56.3	8.2	8.6	7.5	8.3	7.3
	MLP	80.4	27.1	34.4	29.4	21.6	8.2
	CATPlan	80.3	36.7	45.1	31.3	20.0	8.1
VAD	Baseline	61.2	7.8	7.6	7.2	6.8	6.7
	MLP	78.8	17.2	24.0	21.1	14.4	6.7
	CATPlan	92.2	43.2	48.1	45.6	39.5	6.9

Table 2. Classification results on nuScenes validation split for both UniAD and VAD queries. All the values are in percentage, with higher being better.

4.3. Ablation

In this section, we ablate the components of CATPlan and hyper-parameters in Sec. 3.5. All the results in this section are based on UniAD queries on nuScenes. We cache the queries on the nuScenes training split as our training set and the queries on the nuScenes validation split as our test set. A subset of our training set is held out as the validation set, while CATPlan is trained using the rest. We report the ablation results in terms of AP on both the validation and test set. The optimal hyperparameters found apply to the experiments in Sec. 4.1 and Sec. 4.2.

We first study the effect of different numbers of bagging ensembles and the corresponding focal loss. The result is reported in Sec. 4.3. We can see having four bagging ensembles gives the best performance on both the validation set and the test set. We then study the effect of mixup [43] on the top of the bagging ensemble. Mixup is a technique

Ensemble splits	1	2	3	4	6	12
Col:No-Col	1:12	1:6	1:4	1:3	1:2	1:1
α : Ratio	12/13	6/7	4/5	3/4	2/3	1/2
Val AP	63.5	64.4	65.3	66.6	63.9	63.5
Test AP	26.0	26.8	26.9	32.3	31.0	28.2

Table 3. Ablation on number of Bagging Ensembles and α in Focal Loss. No mixup is used during training.

aiming to improve model generalization by training models on convex combinations of pairs of samples and their labels.

There is one hyperparameter α_m that governs the strengths of interpolation between samples-target pairs. The result is reported in Sec. 4.3. As α_m increases, AP keeps improving until the value reaches 3.0. This value is higher than the default value $\alpha_m = 1.0$. The corresponding Beta function is unimodal, which means there is a higher chance of having a mixup coefficient λ close to 0.5 than the default value.

α_m	0.1	0.2	0.3	0.4	0.5	0.6	0.7
Test AP	30.7	32.3	33.4	33.3	33.1	32.8	31.6
Val AP	64.7	64.5	64.7	64.8	64.9	64.8	64.8
α_m	0.8	0.9	1.0	2.0	3.0	4.0	6.0
Test AP	34.5	33.0	35.6	34.7	36.7	35.0	36.4
Val AP	66.1	63.5	67.7	66.8	65.6	65.2	63.2

Table 4. Ablation on α_m for the Beta distribution in Mixup.

We also study the effect of having more layers of transformer decoder. We use the default value $\alpha_m = 1.0$ for the Beta distribution in the mixup. The result is in Sec. 4.3. Surprisingly, adding more transformer decoder layers leads to a performance decrease. We speculate that this could be due to the domain gap, as shown in Sec. 4.4, and that using more transformer layers risks overfitting the training set.

# layers	Mixup			No Mixup		
	1	2	3	1	2	3
Val	67.4	65.9	62.2	66.6	64.2	61.0
Test	35.6	33.0	31.2	32.3	31.4	26.3

Table 5. Ablation on number of decoder layers in CATPlan

4.4. Domain Gap Analysis

In Sec. 4.3, we note the performance on the validation queries is substantially better than on the test queries. During experiments in Sec. 4.1, we also note that the test performance is nearly perfect if we allow training queries and test queries from the same sequence, even if they belong to different scenario types. This indicates that it is the domain gap between different AD video sequences that hinders CATPlan from generalizing and thus causes a drop in the performance on test queries.

In Fig. 3, we use t-SNE algorithm to reduce the dimension of plan queries and visualize them in 2D space. we visualize the planning query h_{plan} from UniAD on nuScenes in both the training and validation split. For the training queries, we assign a color to distinguish collision and non-collision samples. For the test queries, we assign colors based on the test results, true positives, false positives, true negatives, and false negatives.

In Fig. 3a, it is notable that (1) there are two clusters at the top, mixed with training and test samples, and one larger

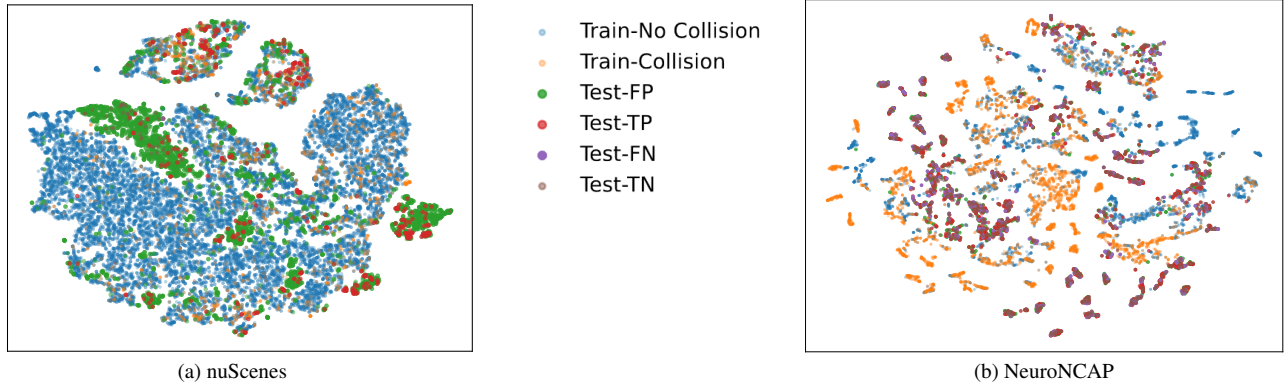


Figure 3. 2D t-SNE plots for plan queries h_{plan} from UniAD on nuScenes and NeuroNCAP. It is better to review in color.

cluster at the bottom, mainly consisting of training samples; (2) there is a hole in the bottom cluster, where happens to be filled with test samples that are FP predictions; (3) there are more TP predictions in the top two clusters, where there seems to be less domain gap between training and test samples. In the supplement, we further visualize the corresponding video sequence of these samples and find that the top-left cluster roughly corresponds to turning right in the video, the top-right cluster roughly corresponds to turning left, and the bottom cluster roughly corresponds to going straight. These findings reveal that the domain gap between the plan and agent queries that correspond to different sequences is significant. The domain gap between nuScenes train and validation splits is the main reason for the performance drop of CATPlan on the test queries. In mixup, setting $\beta = 3.0$ can be treated as a countermeasure to the domain gap since convex combination of sample-target pairs has the potential to alleviate the gap.

In Fig. 3b, we similarly visualize the plan queries h_{plan} on NeuroNCAP, which also exhibit distinct clusters corresponding to different scenario types and sequences. The distribution appears more dispersed than in nuScenes, reflecting the greater variability and discreteness introduced by the simulation environments. In addition, the overlap between training and test samples is relatively low, indicating a significant domain gap between the test and training sets with different scenarios and sequences. These domain gaps become more pronounced when a particular scenario type or sequence has little resemblance to the training distribution. Consequently, CATPlan’s performance declines for queries lying far from learned regions of the feature space.

5. Limitations

We see three main limitations. First, it is acknowledged that end-to-end planners should be evaluated in closed-loop simulation of safety-critical scenarios. To that end, we adopted the SOTA benchmark NeuroNCAP, but it has several limi-

tations, e.g., not being able to model adverse weather conditions, friction, suspension, or deformable objects. Second, the modules in Θ_{target} responsible for detecting and tracking objects sometimes completely fail to detect some agents. This means that there will be no motion query $h_{motion,i}$ for that object, and CATPlan will not account for it. Third, in this work, we do not attempt to divide uncertainty into aleatoric and epistemic. This could, potentially, be achieved by training the target- and loss models on a dataset where some kinds of scenarios are held-out, e.g., particular geographical regions, or certain weather conditions.

6. Conclusion

Ensuring that self-driving vehicles do not lead to heightened road collisions is of paramount importance. In this paper, we presented a lightweight and novel method for predicting collision using hidden embeddings from modern end-to-end AD models. Our method far outperforms the rule-based Gaussian mixture model approaches used as a baseline until now. We designed our CATPlan to make use of transformer queries from the ego-vehicle planning and agent trajectory prediction modules of SOTA end-to-end AD models, and to output the collision loss from said models. This collision loss corresponds nicely to a probability of a collision happening, allowing us to perform binary classification on real-world and simulated autonomous driving datasets.

Our results, while substantial, shine light on a major domain gap in such datasets. Real-world AD datasets do not contain many collision incidents, leading to major data imbalance which sets an potential upper limit to the performance of collision detection. While simulated data is a safer means of gathering collision data, artifacts and hallucinations in the simulations can lead to models learning the dataset rather than generalizable information about the scenes. Despite these limitations, we are confident that our loss prediction transformer approach to collision detection is a major step towards AD vehicles becoming safer.

References

- [1] Adil Kaan Akan and Fatma Güney. Stretchbev: Stretching future instance prediction spatially and temporally. In *European Conference on Computer Vision*, pages 444–460. Springer, 2022. 2
- [2] Lorenzo Bertoni, Sven Kreiss, and Alexandre Alahi. Monoloco: Monocular 3d pedestrian localization and uncertainty estimation. In *Proceedings of the IEEE/CVF international conference on computer vision*, pages 6861–6871, 2019. 2
- [3] Holger Caesar, Varun Bankiti, Alex H Lang, Sourabh Vora, Venice Erin Liong, Qiang Xu, Anush Krishnan, Yu Pan, Giancarlo Baldan, and Oscar Beijbom. nuscenes: A multi-modal dataset for autonomous driving. In *Proceedings of the IEEE/CVF conference on computer vision and pattern recognition*, pages 11621–11631, 2020. 1, 5, 6
- [4] Dian Chen, Vladlen Koltun, and Philipp Krähenbühl. Learning to drive from a world on rails. In *Proceedings of the IEEE/CVF International Conference on Computer Vision*, pages 15590–15599, 2021. 2
- [5] Zhili Chen, Maosheng Ye, Shuangjie Xu, Tongyi Cao, and Qifeng Chen. Ppad: Iterative interactions of prediction and planning for end-to-end autonomous driving. In *Proceedings of the European Conference on Computer Vision (ECCV)*, 2024. 2
- [6] Brian Cheong, Jiachen Zhou, and Steven Waslander. Jdt3d: Addressing the gaps in lidar-based tracking-by-attention. In *European Conference on Computer Vision*, pages 161–177. Springer, 2024. 2
- [7] Felipe Codevilla, Matthias Müller, Antonio López, Vladlen Koltun, and Alexey Dosovitskiy. End-to-end driving via conditional imitation learning. In *2018 IEEE international conference on robotics and automation (ICRA)*, pages 4693–4700. IEEE, 2018. 2
- [8] Nachiket Deo, Eric Wolff, and Oscar Beijbom. Multimodal trajectory prediction conditioned on lane-graph traversals. In *Conference on Robot Learning*, pages 203–212. PMLR, 2022. 2
- [9] Simon Doll, Richard Schulz, Lukas Schneider, Viviane Benzin, Markus Enzweiler, and Hendrik PA Lensch. Spatialdet: Robust scalable transformer-based 3d object detection from multi-view camera images with global cross-sensor attention. In *European Conference on Computer Vision*, pages 230–245. Springer, 2022. 2
- [10] Alexey Dosovitskiy, German Ros, Felipe Codevilla, Antonio Lopez, and Vladlen Koltun. Carla: An open urban driving simulator. In *Conference on robot learning*, pages 1–16. PMLR, 2017. 2
- [11] A. Freytag, E. Rodner, and J. Denzler. Selecting influential examples: Active learning with expected model output changes. In *European Conference on Computer Vision*, pages 562–577. Springer, 2014. 1
- [12] Jakob Gawlikowski, Cedric Rovile Njéutcheu Tassi, Mohsin Ali, Jongseok Lee, Matthias Humt, Jianxiang Feng, Anna Kruspe, Rudolph Triebel, Peter Jung, Ribana Roscher, et al. A survey of uncertainty in deep neural networks. *Artificial Intelligence Review*, 56(Suppl 1):1513–1589, 2023. 2
- [13] Adam W Harley, Zhaoyuan Fang, Jie Li, Rares Ambrus, and Katerina Fragkiadaki. Simple-bev: What really matters for multi-sensor bev perception? In *2023 IEEE International Conference on Robotics and Automation (ICRA)*, pages 2759–2765. IEEE, 2023. 2
- [14] Anthony Hu, Zak Murez, Nikhil Mohan, Sofia Dudas, Jeffrey Hawke, Vijay Badrinarayanan, Roberto Cipolla, and Alex Kendall. Fiery: Future instance prediction in bird’s-eye view from surround monocular cameras. In *Proceedings of the IEEE/CVF International Conference on Computer Vision*, pages 15273–15282, 2021. 2
- [15] Peiyun Hu, Aaron Huang, John Dolan, David Held, and Deva Ramanan. Safe local motion planning with self-supervised freespace forecasting. In *Proceedings of the IEEE/CVF Conference on Computer Vision and Pattern Recognition*, pages 12732–12741, 2021. 2
- [16] Shengchao Hu, Li Chen, Penghao Wu, Hongyang Li, Junchi Yan, and Dacheng Tao. St-p3: End-to-end vision-based autonomous driving via spatial-temporal feature learning. In *European Conference on Computer Vision*, pages 533–549. Springer, 2022. 2
- [17] Yihan Hu, Jiazhi Yang, Li Chen, Keyu Li, Chonghao Sima, Xizhou Zhu, Siqi Chai, Senyao Du, Tianwei Lin, Wenhai Wang, et al. Planning-oriented autonomous driving. In *Proceedings of the IEEE/CVF conference on computer vision and pattern recognition*, pages 17853–17862, 2023. 1, 2, 4, 5, 6
- [18] Xiaosong Jia, Liting Sun, Hang Zhao, Masayoshi Tomizuka, and Wei Zhan. Multi-agent trajectory prediction by combining egocentric and allocentric views. In *Conference on Robot Learning*, pages 1434–1443. PMLR, 2022. 2
- [19] Xiaosong Jia, Penghao Wu, Li Chen, Yu Liu, Hongyang Li, and Junchi Yan. Hdgt: Heterogeneous driving graph transformer for multi-agent trajectory prediction via scene encoding. *IEEE transactions on pattern analysis and machine intelligence*, 45(11):13860–13875, 2023. 2
- [20] Bo Jiang, Shaoyu Chen, Qing Xu, Bencheng Liao, Jiajie Chen, Helong Zhou, Qian Zhang, Wenyu Liu, Chang Huang, and Xinggong Wang. Vad: Vectorized scene representation for efficient autonomous driving. In *Proceedings of the IEEE/CVF International Conference on Computer Vision*, pages 8340–8350, 2023. 1, 2, 3, 5, 6
- [21] Alex Kendall and Yarin Gal. What uncertainties do we need in bayesian deep learning for computer vision? *Advances in neural information processing systems*, 30, 2017. 2
- [22] Tarasha Khurana, Peiyun Hu, Achal Dave, Jason Ziglar, David Held, and Deva Ramanan. Differentiable raycasting for self-supervised occupancy forecasting. In *European Conference on Computer Vision*, pages 353–369. Springer, 2022. 2
- [23] Michael Kirchhof, Bálint Mucsányi, Seong Joon Oh, and Dr Enkelejda Kasneci. URL: A representation learning benchmark for transferable uncertainty estimates. *Advances in Neural Information Processing Systems*, 36:13956–13980, 2023. 2, 3, 4
- [24] Michael Kirchhof, Mark Collier, Seong Joon Oh, and Enkelejda Kasneci. Pretrained visual uncertainties. *arXiv preprint arXiv:2402.16569*, 2024. 3

- [25] Yanwei Li, Zhiding Yu, Jonah Philion, Anima Anandkumar, Sanja Fidler, Jiaya Jia, and Jose Alvarez. End-to-end 3d tracking with decoupled queries. In *Proceedings of the IEEE/CVF International Conference on Computer Vision*, pages 18302–18311, 2023. 2
- [26] Zhiqi Li, Wenhai Wang, Hongyang Li, Enze Xie, Chonghao Sima, Tong Lu, Qiao Yu, and Jifeng Dai. Bevformer: Learning bird’s-eye-view representation from multi-camera images via spatiotemporal transformers, 2022. 2
- [27] Tsung-Yi Lin, Priya Goyal, Ross Girshick, Kaiming He, and Piotr Dollár. Focal loss for dense object detection. In *Proceedings of the IEEE international conference on computer vision*, pages 2980–2988, 2017. 5
- [28] Yingfei Liu, Tiancai Wang, Xiangyu Zhang, and Jian Sun. Petr: Position embedding transformation for multi-view 3d object detection. In *European conference on computer vision*, pages 531–548. Springer, 2022. 2
- [29] William Ljungbergh, Adam Tonderski, Joakim Johnander, Holger Caesar, Kalle Åström, Michael Felsberg, and Christoffer Petersson. Neuroncap: Photorealistic closed-loop safety testing for autonomous driving. In *European Conference on Computer Vision*, pages 161–177. Springer, 2024. 1, 5
- [30] Isak Meding, Alexander Bodin, Adam Tonderski, Joakim Johnander, Christoffer Petersson, and Lennart Svensson. You can have your ensemble and run it too-deep ensembles spread over time. In *Proceedings of the IEEE/CVF International Conference on Computer Vision*, pages 4020–4029, 2023. 2
- [31] Tim Meinhardt, Alexander Kirillov, Laura Leal-Taixe, and Christoph Feichtenhofer. Trackformer: Multi-object tracking with transformers. In *Proceedings of the IEEE/CVF conference on computer vision and pattern recognition*, pages 8844–8854, 2022. 2
- [32] Ziqi Pang, Jie Li, Pavel Tokmakov, Dian Chen, Sergey Zagoruyko, and Yu-Xiong Wang. Standing between past and future: Spatio-temporal modeling for multi-camera 3d multi-object tracking. In *Proceedings of the IEEE/CVF conference on computer vision and pattern recognition*, pages 17928–17938, 2023. 2
- [33] Aditya Prakash, Kashyap Chitta, and Andreas Geiger. Multi-modal fusion transformer for end-to-end autonomous driving. In *Proceedings of the IEEE/CVF conference on computer vision and pattern recognition*, pages 7077–7087, 2021. 2
- [34] Avishkar Saha, Oscar Mendez, Chris Russell, and Richard Bowden. Translating images into maps. In *2022 International conference on robotics and automation (ICRA)*, pages 9200–9206. IEEE, 2022. 2
- [35] B. Settles. Active learning literature survey. Technical report, University of Wisconsin-Madison Department of Computer Sciences, 2009. 1
- [36] Adam Tonderski, Carl Lindström, Georg Hess, William Ljungbergh, Lennart Svensson, and Christoffer Petersson. Neurad: Neural rendering for autonomous driving. In *Proceedings of the IEEE/CVF Conference on Computer Vision and Pattern Recognition*, pages 14895–14904, 2024. 5
- [37] Hristos Tyrallis and Georgia Papacharalampous. A review of predictive uncertainty estimation with machine learning. *Artificial Intelligence Review*, 57(4):94, 2024. 2
- [38] Theodor Westny, Erik Frisk, and Björn Olofsson. Vehicle behavior prediction and generalization using imbalanced learning techniques. In *2021 IEEE International Intelligent Transportation Systems Conference (ITSC)*, pages 2003–2010. IEEE, 2021. 4
- [39] Penghao Wu, Li Chen, Hongyang Li, Xiaosong Jia, Junchi Yan, and Yu Qiao. Policy pre-training for autonomous driving via self-supervised geometric modeling. In *11th International Conference on Learning Representations, ICLR 2023*, 2023. 2
- [40] Donggeun Yoo and In So Kweon. Learning loss for active learning. In *Proceedings of the IEEE/CVF conference on computer vision and pattern recognition*, pages 93–102, 2019. 1, 2, 3, 4
- [41] Linlin Yu, Bowen Yang, Tianhao Wang, Kangshuo Li, and Feng Chen. Predictive uncertainty quantification for bird’s eye view segmentation: A benchmark and novel loss function. In *The Thirteenth International Conference on Learning Representations*. 2
- [42] Xuanlong Yu, Gianni Franchi, Jindong Gu, and Emanuel Aldea. Discretization-induced dirichlet posterior for robust uncertainty quantification on regression. In *Proceedings of the AAAI Conference on Artificial Intelligence*, pages 6835–6843, 2024. 3
- [43] Hongyi Zhang, Moustapha Cisse, Yann N Dauphin, and David Lopez-Paz. mixup: Beyond empirical risk minimization. *arXiv preprint arXiv:1710.09412*, 2017. 7
- [44] Yang Zhao, Xiao Wang, and Hong Cheng. Radar-image fusion transformer for object detection with uncertainty estimation. In *2023 IEEE 26th International Conference on Intelligent Transportation Systems (ITSC)*, pages 814–819. IEEE, 2023. 2
- [45] Wenzhao Zheng, Ruiqi Song, Xianda Guo, Chenming Zhang, and Long Chen. Genad: Generative end-to-end autonomous driving. In *Proceedings of the European Conference on Computer Vision (ECCV)*, 2024. 2, 5
- [46] Jian Zhou, Björn Olofsson, and Erik Frisk. Interaction-aware motion planning for autonomous vehicles with multi-modal obstacle uncertainties using model predictive control. *IEEE Transactions on Intelligent Vehicles*, 9(1), 2023. 4